Inelastic electron scattering to negative parity states of ^{24}Mg

H. Zarek, S. Yen, B. O. Pich, and T. E. Drake
Department of Physics, University of Toronto, Toronto, Ontario, Canada M5S 1A7

C. F. Williamson, S. Kowalski, and C. P. Sargent
Bates Linear Accelerator and Department of Physics, Massachusetts Institute of Technology, Cambridge, Massachusetts 02139

(Received 20 January 1984)

The electromagnetic form factors for the stronger transitions to negative parity states in ^{24}Mg were measured for electron energies 90—280 MeV and scattering angles of 90° and 160°. The isoscalar $K^\pi=0^-$ and 3^- bands show form factors in agreement with open-shell random-phase approximation calculations, even though the parentages of these two bands are radically different. For the isovector negative parity states, a quenching of magnetic strength is observed; its origins are discussed.

I. INTRODUCTION

In a recent paper, Yen *et al.*[1] studied the negative-parity states of ^{28}Si with inelastic electron scattering, and compared the experimental form factors with the predictions of the open-shell random phase approximation (OSRPA) of Rowe and Wong.[2] They found that the results were very sensitive to the one- and two-particle densities of the ground state wave function, and that several different ground states were needed to reproduce the observed form factors. It was suggested that this may be due to the fact that the ^{28}Si nucleus is relatively soft to shape deformations, with the result that the electroexcitation of a single nucleon may be coupled to a change in the configuration of the remaining core nucleons from oblate to prolate.

It is thus interesting to inquire what the situation is in a rigidly prolate nucleus like ^{24}Mg, where the electroexcitation of a single nucleon is not expected to lead to a drastic change in the average field of the remaining nucleons. Can a shell model ground state, operated on by the OSRPA, yield the form factors of the excited states of the nucleus? The experimental evidence to be presented in this paper suggests that it can.

II. EXPERIMENT

The experiments were performed with the high-resolution electron-scattering facility at the MIT-Bates linear accelerator.[3] A typical spectrum of inelastically-scattered electrons is shown in Fig. 1. The targets used were foils of 99.4% ^{24}Mg, of area 4.5 cm×4.0 cm. Absolute measurements of the cross sections were made at several momentum transfers between 0.9 and 2.6 fm^{-1}. Typical beam currents were 8—20 μA for $\theta=90°$, and 15—35 μA for $\theta=160°$. Corrections were made for detector dead time.

The differential cross section for inelastic electron scattering from a target nucleus of mass M_T to an isolated resonance is related to the electromagnetic form factors in the plane-wave Born approximation (PWBA) by

$$\frac{d\sigma}{d\Omega}=\sigma_m\eta_R\left[F_{C\lambda}^2(q)+\left[\tfrac{1}{2}+\tan^2\frac{\theta}{2}\right]F_{T\lambda}^2(q)\right],$$

where $d\sigma/d\Omega$ is the cross section with radiative correction applied,

$$\sigma_m=\frac{Z^2\alpha^2\cos^2\theta/2}{4E_i^2\sin^4\theta/2}$$

is the Mott cross section,

$$\eta_R=[1+(2E_i/M_T)\sin^2\tfrac{1}{2}\theta]^{-1}$$

is a recoil correction factor, E_i is the incident electron energy, q is the three-momentum transfer, $F_{C\lambda}^2(q)$ is the Coulomb squared form factor, and $F_{T\lambda}^2(q)$ is the transverse squared form factor.

We further define the total squared form factor

$$F^2(q)=\frac{d\sigma/d\Omega}{\sigma_m\eta_R}\ .$$

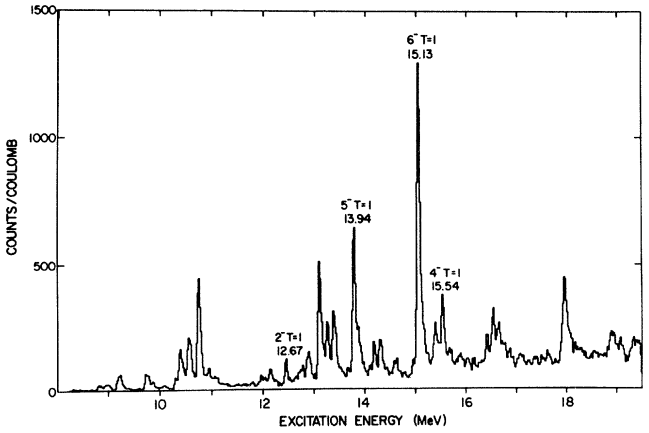

FIG. 1. Spectrum of electrons scattered from a ^{24}Mg target. The incident electron energy is 194 MeV, and the scattering angle is $\theta=160°$.

Note that the squared form factors in this paper are smaller than those defined by Yen *et al.*[1] by a factor of $4\pi/Z^2$. Since the electron is accelerated by the Coulomb field of the target nucleus, the effective momentum transfer is actually greater than q given above, and is approximately

$$q_{\text{Born}}=q\left[1+\frac{4}{3}\frac{Z\alpha}{1.05A^{1/3}E_i}\right].$$

For each resonance we present a plot of $F^2(q_{\text{Born}})$ vs q_{Born}, and this is compared with the theoretical PWBA squared form factor. For a purely transverse excitation, the ratio

$$R=F^2(q,\theta=160°)/F^2(q,\theta=90°)$$

is equal to 21.8, while for a pure Coulomb excitation, $R=1.0$.

III. OSRPA CALCULATIONS

Theoretical form factors for the negative parity states of ^{24}Mg have been calculated using the open-shell random phase approximation (OSRPA) of Rowe and Wong.[2] In the OSRPA, for a $J=T=0$ nucleus, an excited state $|\chi\rangle$ is obtained from the uncorrelated ground state $|\phi_0\rangle$ by application of an excitation operator $O^\dagger_\lambda$

$$|\chi\rangle=O^\dagger_\lambda|\phi_0\rangle\ ,$$

where

$$O^\dagger_\lambda=\sum_{p>h}(n_h-n_p)^{-1/2}[Y_{ph}(\lambda)A^\dagger_{ph}-Z_{ph}(\lambda)A_{ph}]\ ,$$

p and h are particle and hole orbitals, respectively; n_p and n_h are the fractional occupancies of these orbitals; $A^\dagger_{ph}$ and A_{ph} are the particle-hole creation and destruction operators, respectively; and Y_{ph} and Z_{ph} are the forward and backward amplitudes for particle-hole creation and destruction, respectively. If we define the normalized amplitudes

$$F_{ph}=(n_h-n_p)^{1/2}\hat{T}^{-1}Y^*_{ph}\ ,$$
$$F_{hp}=(n_h-n_p)^{1/2}(-1)^{p-h+J+T}Z^*_{ph}\ ,$$

then the reduced matrix element for any one-body operator $W^J=\sum_T W^{JT}$ is given by

$$\langle J_f||W^J||J_i\rangle=\hat{J}_i\sum_{\mu\nu T}F_{\mu\nu}(JT)\langle\mu|||W^{JT}|||\nu\rangle\ ,$$

where

$$\hat{J}\equiv(2J+1)^{+1/2},\quad \hat{T}=(2T+1)^{+1/2}\ ,$$

and T is the isospin of the final state. Thus all of the nuclear structure information is contained in the amplitudes $F_{\mu\nu}$.

The OSRPA has a great advantage over conventional shell models in that the dimension of the matrix to be diagonalized is equal to the number of particle-hole excitations which can couple to the desired J and T, and not to the number of nucleon configurations, which is generally much larger. In this investigation, the active excitation space consists of all $p\rightarrow sd$ and $sd\rightarrow fp$ shell one-particle–one-hole excitations.

TABLE I. Fractional occupancies and single particle energies.

Orbital	Energy	Occupancy (Kuo)	Occupancy (Wildenthal)
$1p_{3/2}$	−8.3070	1.0	1.0
$1p_{1/2}$	−3.5331	1.0	1.0
$1d_{5/2}$	4.6455	0.41714	0.4787
$2s_{1/2}$	6.4875	0.2861	0.2310
$1d_{3/2}$	10.4993	0.2314	0.1664
$1f_{7/2}$	15.9325	0.0	0.0
$2p_{3/2}$	17.7426	0.0	0.0
$2p_{1/2}$	20.7087	0.0	0.0
$1f_{5/2}$	24.7127	0.0	0.0

The ground state wave function for ^{24}Mg employed in this investigation was calculated with the Oak Ridge-Rochester shell model code[4] for an active $(sd)^8$ configuration and an inert ^{16}O core. Renormalized Kuo matrix elements,[5] derived from the Hamada-Johnston potential, were used for the interaction Hamiltonian. The *sd* shell fractional occupancies were obtained from the shell model calculation. In the uncorrelated ground state, all orbitals below the *sd* shell are assumed to be fully occupied, and all orbitals above the *sd* shell are assumed to be completely empty. The single particle energies for ^{24}Mg were interpolated from the single particle energies in ^{17}O and ^{41}Ca using the interpolation procedure of Ref. 6. The fractional occupancies and single particle energies are listed in Table I. For comparison, we also list the occupancies given by the shell model calculations of Wildenthal, which use two-body matrix elements fitted to data over the entire *sd* shell.

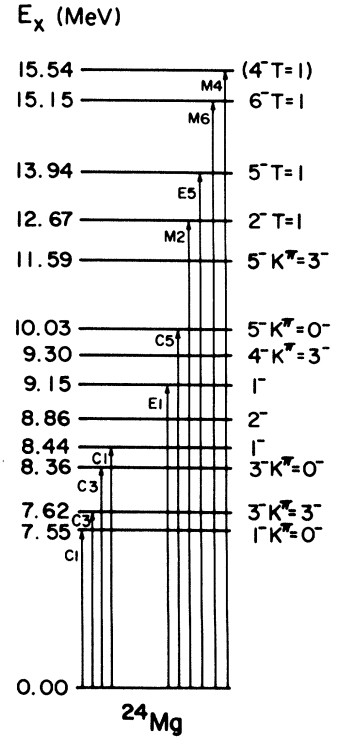

FIG. 2. Level scheme of prominent negative-parity states of ^{24}Mg.

In all OSRPA calculations described in this paper, harmonic oscillator wave functions with an oscillator parameter of $b=1.82$ fm were used, and both the center of mass correction for shell model wave functions and the finite nucleon size correction were applied. The two-body interaction used is essentially the CAL interaction of Gillet and Sanderson,[7] the parameters for which are listed in Ref. 1.

The spins, parities, K-band assignments, and excitation energies of the states to be studied in this paper are shown in Fig. 2.

IV. EXPERIMENTAL AND THEORETICAL RESULTS

A. 3^- $T=0$ states

The lowest two 3^- $T=0$ states in ^{24}Mg occur at excitation energies of 7.616 and 8.358 MeV.[8] The 3_1^- state corresponds to the bandhead of the $K=3$ band, and has been resolved in electron scattering for the first time from the nearby 1^- state at 7.553 MeV. The 3_2^- state is the second member of the $K=0$ band. Since different K bands have different intrinsic states, one would expect the 3_1^- and 3_2^- to have different particle-hole parentages. The squared form factors for these two states are plotted in Fig. 3. A comparison of $F^2(q)$ at $\theta=90°$ and $\theta=160°$ reveals that the transverse contribution to $F^2(q)$ is negligible, in agreement with the OSRPA calculations. The very different shapes of $F^2(q)$ for the two 3^- states indicate that these states are indeed different, with the 3_2^- state having a much larger transition radius than the 3_1^- state.

Also shown in Fig. 3 are the OSRPA results for two 3^- states. The OSRPA squared form factor for the 3_1^- state must be reduced by 1.7 to bring it into agreement with the experimental results, but no renormalization is required for the 3_2^- state; in both cases the OSRPA successfully predicts the shape of $F^2(q)$. As shown in Table II and Fig. 4, the predominant amplitudes for the 3_1^- state consist of particle-hole excitations from the p shell into the sd shell, whereas the 3_2^- state is more heavily mixed, with major components characterized by excitations into the fp shell. This structure is qualitatively corroborated by the work of Tribble, Garvey, and Comfort.[9] These workers measured a larger ^{25}Mg(p,d) pickup strength to the 3_1^- state in ^{24}Mg than to the 3_2^-, which indicates that the 3_1^- has a larger "hole" component, as expected for an excitation from the p to the sd shell. On the other hand, they measured a larger ^{23}Na(^{3}He,d) stripping strength to the

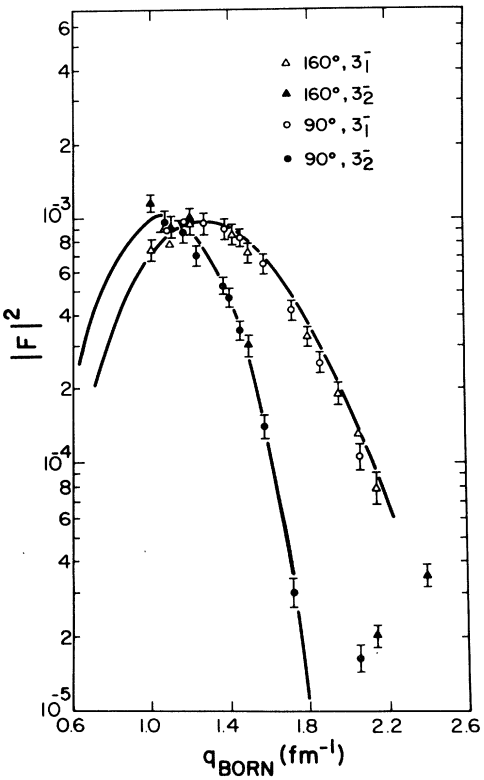

FIG. 3. Total squared form factors for the 3_1^- (7.62) and 3_2^- (8.36) states of ^{24}Mg.

TABLE II. Configurations for 3^- $T=0$ in ^{24}Mg.

Configuration number	Particle	Hole
1	$1d_{5/2}$	$1p_{3/2}$
2	$1d_{5/2}$	$1p_{1/2}$
3	$1d_{3/2}$	$1p_{3/2}$
4	$1f_{7/2}$	$1d_{5/2}$
5	$1f_{7/2}$	$1d_{3/2}$
6	$1f_{7/2}$	$1s_{1/2}$
7	$1f_{5/2}$	$1d_{5/2}$
8	$1f_{5/2}$	$1d_{3/2}$
9	$1f_{5/2}$	$2s_{1/2}$
10	$2p_{3/2}$	$1d_{5/2}$
11	$2p_{3/2}$	$1d_{3/2}$
12	$2p_{1/2}$	$1d_{5/2}$

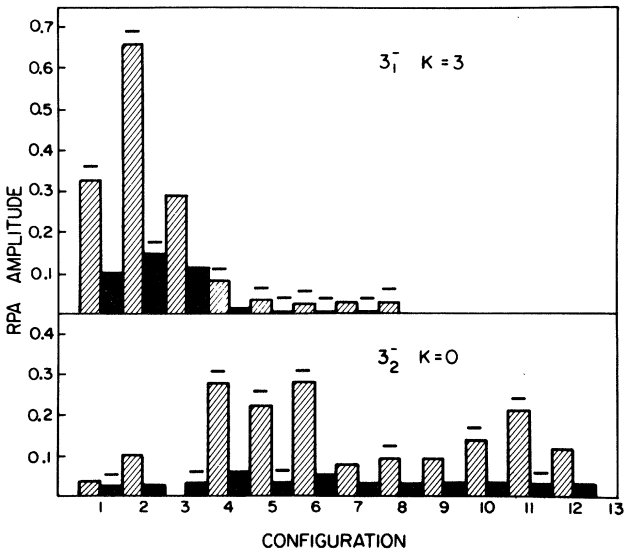

FIG. 4. RPA amplitudes for the 3_1^- and 3_2^- OSRPA states of ^{24}Mg. A shell-model ground state calculated with renormalized Kuo matrix elements was used. The particle-hole configurations 1–12 correspond to those listed in Table II. Forward amplitudes F_{ph} are represented by hatched bars, backward amplitudes F_{hp} by solid bars. The height of the bar represents the magnitude of F_{ph} or F_{hp}. A minus sign over a bar denotes a negative amplitude.

3_2^- state in ^{24}Mg than to the 3_1^- state, which indicates that the 3_2^- has a large "particle" component, as expected for an excitation into the fp shell.

The theoretical and experimental excitation energies, and the experimental $B(C3)$ values, are listed in Table III.

In Ref. 1 it was shown that for ^{28}Si, a single model ground state could not reproduce the shapes of both the 3_1^- and 3_2^- form factors, and that the form factor was sensitive to the model ground state used. This was attributed to the softness of the ^{28}Si nucleus to oblate-prolate configuration changes, and the 3_1^- was conjectured to be oblate and the 3_2^- prolate. The ^{24}Mg nucleus, by contrast, is rigidly prolate, so that the average field of the nucleus does not change shape when a particle-hole pair is excited from the ground state. Thus, a single model ground state is able to predict the shapes of both the 3_1^- and 3_2^- in ^{24}Mg. For the 3^- states of ^{24}Mg we have also performed OSRPA calculations using a model ground state computed using the shell model of Wildenthal,[10] the occupancies of which are tabulated in Table I. The results are almost identical to the ones already presented.

B. 5^- $T=0$ state

The 5^- $T=0$ state is interesting because it is the simplest negative- and natural-parity isoscalar excitation possible in the model space of the p, ds and fp shells. As such, it should be an excellent test of the OSRPA, since it is immune to meson exchange currents which could affect even simple spin excitations like the 6^- $T=1$.

A 5^- state has been identified in our (e,e') spectra at an excitation energy of $E_x=10.030\pm0.030$ MeV. A 5^- $T=0$ state has been found in the ^{12}C(^{16}O,α)^{24}Mg experiment of Branford *et al.*[11] at $E_x=10.027$ MeV; these authors suggest that this state belongs to the $K=0$ band. The spin assignment is corroborated by the ^{24}Mg(p,p') work of Zwieglinski *et al.*[12] The experimental squared form factor is displayed in Fig. 5. For $q<1.4$ fm^{-1}, the shape of the form factor is distorted by the contribution of the nearby 2^+ $T=1$ state at $E_x=10.059$ MeV.[8] There is no measurable transverse component to the squared form factor.

The OSRPA predicts the lowest 5^- $T=0$ state in ^{24}Mg to lie at 10.38 MeV. The squared form factor is predicted to be predominantly Coulomb: at $q_{\rm Born}=1.7$ fm^{-1}, the OSRPA predicts $F_C^2(q)=2.86\times10^{-4}$, $F_T^2(q)=4.34\times10^{-7}$. The calculation must be reduced by 0.85 to fit the data, but the shape is in agreement with the data. The predicted parentage of this state is tabulated in Table IV. It is interesting that the 3_2^- also has predominant $1f_{7/2}$-$1d_{5/2}{}^{-1}$ and $1f_{7/2}$-$1d_{3/2}{}^{-1}$ configurations. This is exactly what one would expect if the different members of a K band have similar intrinsic states, and is evidence that the 3_2^- and 5_1^- are both members of the same K band.

On the basis of the OSRPA calculation, renormalized to fit the data, the extrapolated $B(C5)$ value for this state is 2.5×10^5 e^2fm^{10}.

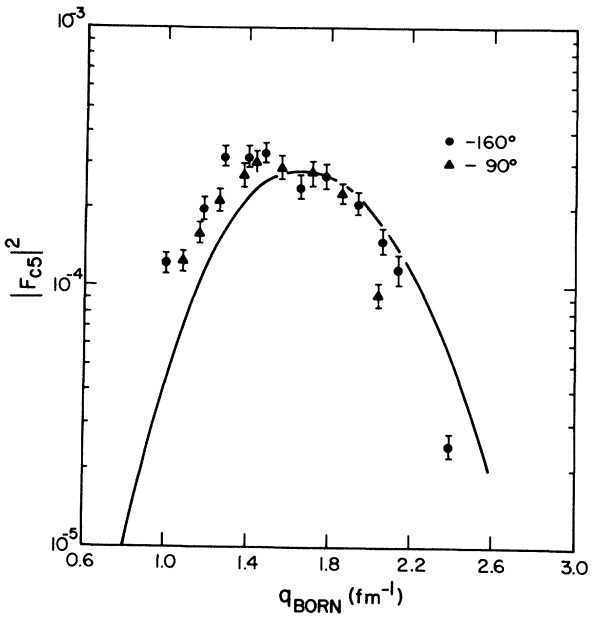

FIG. 5. Total squared form factor for $\theta=160°$ and $\theta=90°$ for the 5^- $T=0$ (10.03 MeV) state. The solid line is the predicted Coulomb squared form factor.

C. 1^- $T=0$ states

Three 1^- $T=0$ states have been identified at excitation energies of 7.553, 8.438, and 9.148 MeV. None of these states has been previously resolved in (e,e').

The 1_1^- (7.553) state is the bandhead of the $K=0$ band. The experimental data displayed in Fig. 6 show $F^2(q)$ to be predominantly Coulomb. The OSRPA is unable to predict the shape of $F^2(q)$ for this state; it predicts a diffraction minimum at the wrong q. The reason for this failure will be discussed shortly.

The 1_2^- (8.438) state cannot be resolved from the nearby $(3,4)^+$ (8.437) state. However, the 1^- (8.438) state has a large γ-ray branching ratio to the ground state (82%),[8] whereas the $(3,4)^+$ (8.437) state has no measurable γ decay to the ground state ($<2\%$).[8] This suggests that the 1^- state would be much more strongly excited in (e,e') than would the $(3,4)^+$ state. A 3^+ state would exhibit a purely transverse squared form factor; the absence of a large transverse component in the experimental data rules out a large contribution from a 3^+ state. If the 8.437

TABLE III. $B(C3)$ values and excitation energies.

State	$B(C3)$ (e^2fm^6)	E_x (theory) (MeV)	E_x (experiment) (MeV)
3_1^-	5.62×10^2	7.658	7.616
3_2^-	1.58×10^3	10.067	8.358

TABLE IV. Predicted parentage of 5^- $T=0$.

Configuration	F_{ph} (fore)	F_{np} (back)
$1f_{7/2}$-$1d_{5/2}$	0.21862	−0.03792
$1f_{7/2}$-$1d_{3/2}$	0.44844	0.05323
$1f_{5/2}$-$1d_{5/2}$	−0.12327	−0.04273

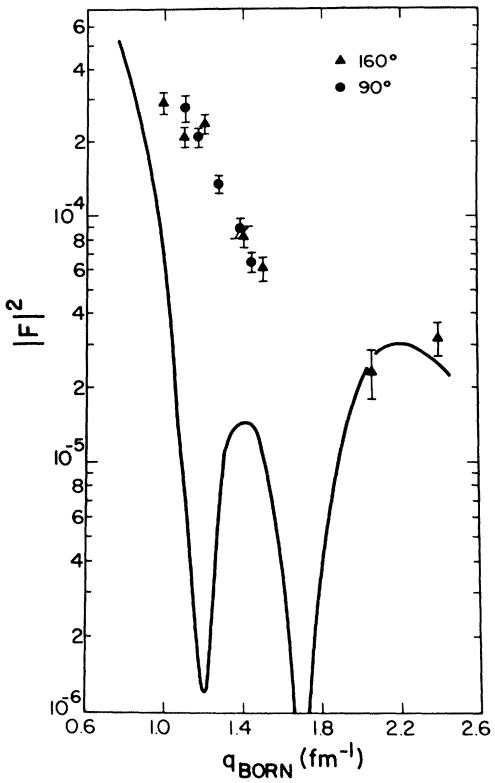

FIG. 6. Total squared form factor for $\theta=160°$ and $\theta=90°$ for the 1_1^- $T=0$ (7.553 MeV) state. The solid line is the predicted OSRPA Coulomb squared form factor.

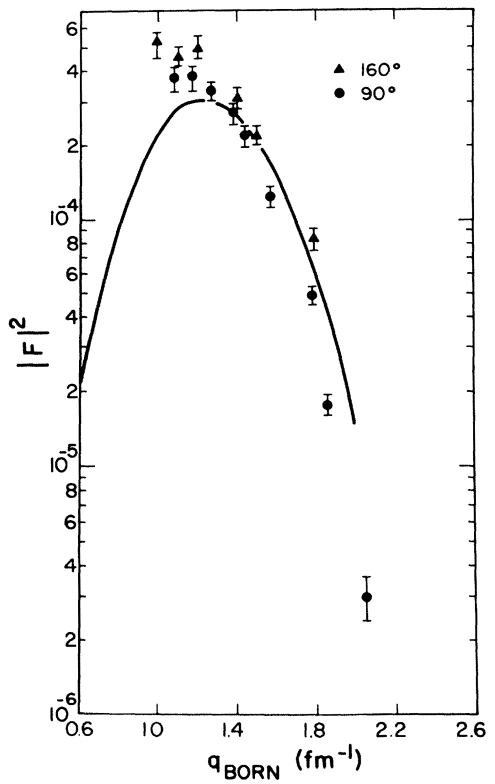

FIG. 7. Total squared form factor for the 1_2^- $T=0$ (8.438 MeV) state. The solid line is the predicted OSRPA squared form factor for $\theta=90°$, reduced by the factor 0.53.

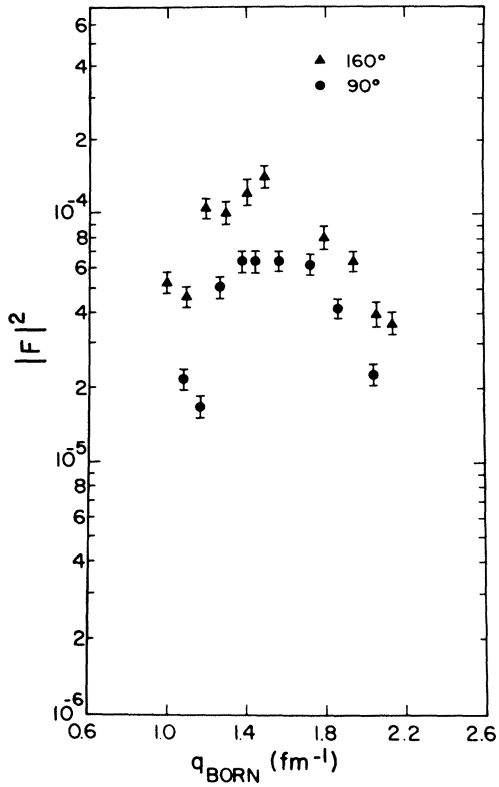

FIG. 8. Total squared form factor for the 1_3^- $T=0$ (9.148 MeV) state.

state were 4^+, it could contribute significantly to the experimental squared form factor. However, the shell model calculations of Brown, Chung, and Wildenthal[13] predict the 4_3^+ in ^{24}Mg to be weak, with a maximum $F^2(q)$ of only 2.97×10^{-5} occurring at $q=1.50$ fm^{-1}. Thus we conclude that the peak observed in electron scattering is probably dominated by the 1_2^- state. As shown in Fig. 7, the OSRPA is able to roughly predict the shape of the 1_2^-, but a renormalization factor of 0.53 is necessary.

The data for the 1_3^- state are displayed in Fig. 8. The OSRPA is again completely unable to predict either the size or shape of $F^2(q)$ (not shown in Fig. 8), and moreover predicts a large, order-of-magnitude enhancement of F^2 ($\theta=160°$) over F^2 ($\theta=90°$).

The likely reason for the failure of the OSRPA for the 1^- $T=0$ states is that the solutions contain the spurious center-of-mass motion. Ideally, for a translationally invariant Hamiltonian, the spurious solutions of the random phase approximation (RPA) should occur at zero energy,[14] but for realistic Hamiltonians, spurious components are mixed into the solutions of nonzero energy.

D. 6^- $T=1$ state

The strongest peak in the (e,e') spectrum at $\theta=160°$ and $q>1.4$ fm^{-1} has been identified as a 6^- $T=1$ state on the basis of comparison with OSRPA predictions.[15] The excitation energy of this resonance is 15.130 ± 0.040 MeV; the value reported in Ref. 15 was incorrect. The total squared form factor is shown in Fig. 9; no Coulomb contribution

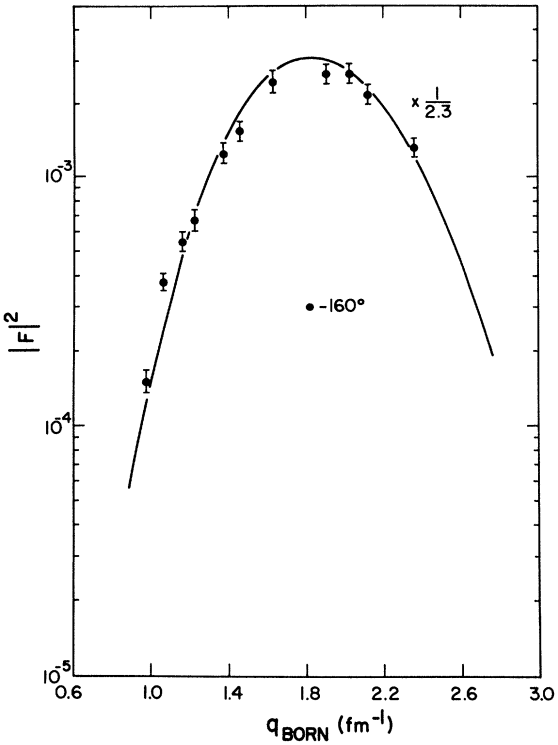

FIG. 9. Total squared form factor for the 6^- $T=1$ state. The solid line is the OSRPA calculation reduced by a factor of 2.3.

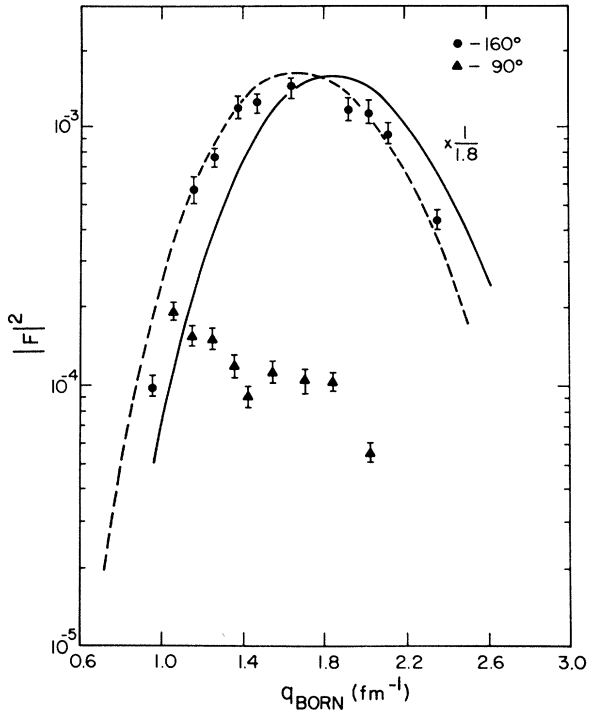

FIG. 10. The tentative 5^- $T=1$ state. The dashed curve is the Coulomb squared form factor for the first OSRPA 5^- $T=1$ state, scaled up by a factor of 17.5 for comparison with the 160° data. The solid curve is the total squared form factor, scaled down by a factor of 1.8. This state is poorly resolved at $\theta=90°$.

is observed. The experimental $B(M6)$ value is 2.4×10^8 $e^2\,\mathrm{fm}^{12}$.

In the model space of the calculation, only the $1f_{7/2}$-$1d_{5/2}{}^{-1}$ particle-hole configuration can contribute to the 6^- $T=1$. The predicted OSRPA amplitudes are F_{ph} (fore)$=0.373$, F_{hp} (back)$=0.0097$, and the predicted excitation energy is 17.6 MeV. The OSRPA predicts a squared form factor which is of the correct shape, but which is too large by a factor of 2.3.

The quenching of magnetic strength, seen here for the 6^- $T=1$ state, is a widely-observed phenomenon[16] for which there is yet no definitive explanation. Some authors[17,18] have attributed the quenching to many-particle, many-hole components in the wave function of the physical 6^- $T=1$ state, which cannot be excited by a one-body operator such as the electromagnetic operator. If this is the explanation, it is difficult to see why the quenching factor should be close to 0.5 for ^{24}Mg, ^{28}Si,[1,15,19] and ^{208}Pb,[20,21] since these nuclei have different structures and thus presumably different many-particle—many-hole content. Other suggested explanations are meson exchange currents[16,22,23] and excitation of Δ-hole pairs.[24–26] The observed quenching may in fact be due to a combination of all of these effects, and the best place to search for these effects is in states like the 6^- $T=1$ where the "conventional" structure consists of simply one particle-hole configuration.

E. 5^- $T=1$ state

A resonance observed at 13.930 ± 0.050 MeV has the total squared form factor shown in Fig. 10. It is tentatively given a spin-parity assignment of 5^- $T=1$ based on comparison with the OSRPA predictions. A 5^- state has been previously identified at 13.86 MeV.[11] The following evidence points to a 5^- $T=1$ assignment.

The OSRPA predicts a 5^- $T=1$ state at 14.7 MeV, only 0.8 MeV higher than the experimental excitation energy. At $q_{\mathrm{eff}}\approx1.7$ fm^{-1}, the ratio $R=F^2$ (160°)$/F^2$(90°) is observed to be 14.1 ± 0.7, whereas the OSRPA predicts $R=13.0$. As shown in Fig. 10, the theoretical total squared form factor must be reduced by 1.8 to bring it into rough agreement with experiment. However, the squared form factor is predicted to peak at $q_{\mathrm{eff}}=1.8$ fm^{-1}, whereas experimentally, it peaks at $q_{\mathrm{eff}}=1.7$ fm^{-1}. Figure 10 shows that the Coulomb form factor alone has the correct shape to fit the data; the addition of the transverse part shifts the OSRPA form factor to higher q.

Three 5^- $T=1$ states can be constructed in the model space used in this study. The pertinent data for these states are summarized in Tables V and VI. The second 5^- $T=1$ state is predicted to have a predominant $1f_{7/2}$-

TABLE V. Characteristics of 5^- $T=0$ OSRPA states (predicted).

State	E_x (MeV)	$B(E5)$ $e^2\,\mathrm{fm}^{10}$	Dominant configuration
1	14.661	9.623×10^4	$1f_{7/2}$-$1d_{3/2}{}^{-1}$
2	19.128	5.910×10^4	$1f_{7/2}$-$1d_{5/2}{}^{-1}$
3	26.920	2.017×10^5	$1f_{5/2}$-$1d_{5/2}{}^{-1}$

TABLE VI. 5^- $T=1$ state parentage (first OSRPA state).

Configuration	F_{ph} (fore)	F_{hp} (back)
$1f_{7/2}$-$1d_{5/2}{}^{-1}$	−0.04163	−0.00667
$1f_{7/2}$-$1d_{3/2}{}^{-1}$	−0.27577	−0.00003
$1f_{5/2}$-$1d_{5/2}{}^{-1}$	−0.01999	0.01169

$1d_{5/2}{}^{-1}$ configuration, with its transverse form factor peaking at 1.3 fm^{-1}. Therefore, adjustment of the $1f_{7/2}$-$1d_{5/2}{}^{-1}$ admixture in the first 5^- state would bring its squared form factor into closer agreement with experiment. The strongest 5^- $T=1$ state is predicted to lie at an excitation energy of 26.9 MeV, but at such a high excitation energy, the state would be broadened by particle emission and would not be resolved above the background. The parentages of the three OSRPA 5^- states are summarized in Table V.

F. 4^- $T=1$ state

In the *p-sd-fp* model space used in this study, a total of seven 4^- $T=1$ states can be formed from one-particle one-hole excitations. The OSRPA prediction for the strong second lowest-energy state is shown in Fig. 11.

An excited state is found in the (e,e′) spectrum at (15.540±0.060) MeV, and this has been tentatively assigned as 4^- $T=1$ on the basis of comparison with the OSRPA results. The experimental total squared form factor is displayed in Fig. 11. The $\theta=160°$ data are enhanced by a factor of $R=(22\pm1)$ over the $\theta=90°$ data, which indicates that this resonance is a pure magnetic excitation. A comparison of the shapes of the OSRPA squared form factors with the data shows that only the second OSRPA 4^- $T=1$ state has the correct shape. The predicted energy of 17.88 MeV is too high by 2.34 MeV. This is approximately the same as the difference between the calculated and experimental energies for the 6^- $T=1$ resonance. The OSRPA squared form factor must be reduced by a factor of 5.6 to bring it into agreement with the experimental data. This reduction factor is far larger than is needed for any other $T=1$ resonance studied in this work, and might be attributed to a fragmentation of the one-particle—one-hole strength due to coupling with

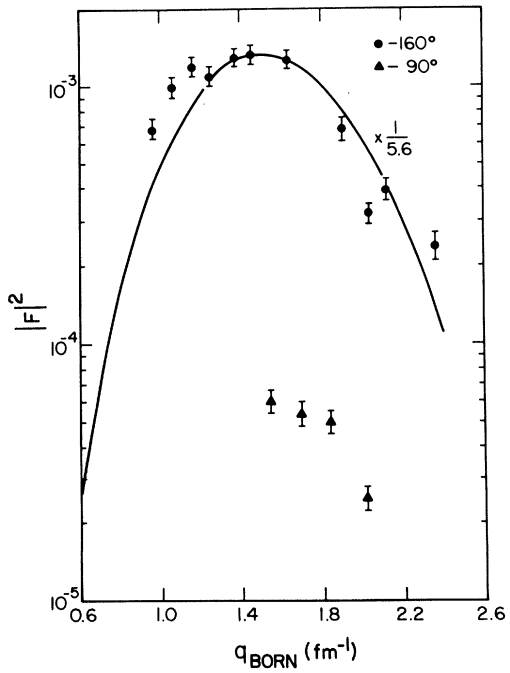

FIG. 11. A tentative 4^- $T=1$ state. The solid curve denotes the total squared form factor at $\theta=160°$ for the second OSRPA 4^- $T=1$ state. A reduction factor of 5.6 is required to fit the data.

TABLE VII. OSRPA amplitudes for the tentative 4^- $T=1$ before renormalization to fit the data; $B(M4)=4.1\times10^3$ e^2fm^8.

Configuration	F_{ph} (fore)	F_{hp} (back)
$1d_{5/2}$-$1p_{3/2}{}^{-1}$	0.4397	0.0158
$1f_{7/2}$-$1d_{5/2}{}^{-1}$	−0.0260	0.0124
$1f_{7/2}$-$1d_{3/2}{}^{-1}$	−0.0070	0.0082
$1f_{7/2}$-$2s_{1/2}{}^{-1}$	0.0127	0.0084
$1f_{5/2}$-$1d_{5/2}{}^{-1}$	−0.0029	−0.0035
$1f_{5/2}$-$1d_{3/2}{}^{-1}$	0.0023	−0.0012
$2p_{3/2}$-$1d_{5/2}{}^{-1}$	0.0150	0.0021

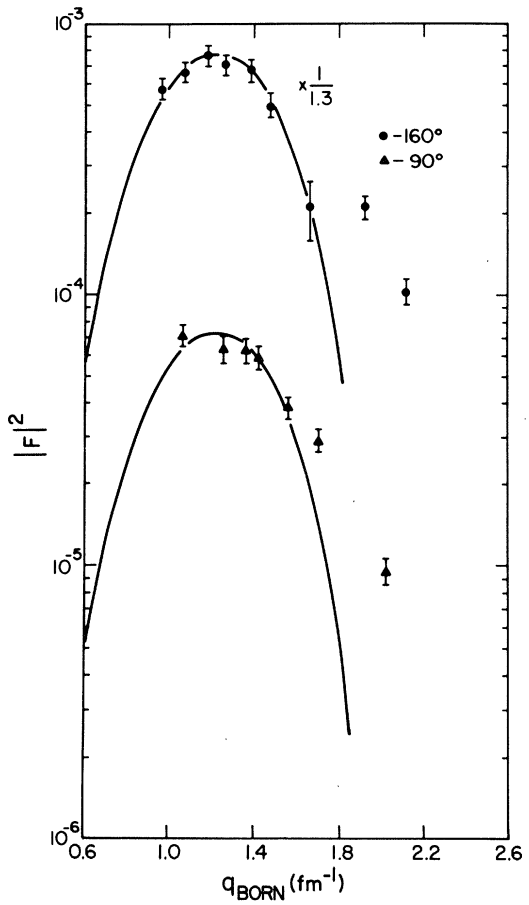

FIG. 12. Total squared form factors for the 2^- $T=1$ state at $E_x=12.640$ MeV. The solid curves denote the calculations for the lowest OSRPA 2^- $T=1$ state. The curve for $\theta=160°$ has been reduced by a factor of 1.3 to fit the data. Theory predicts an enhancement factor of $R=21.8$, but the observed factor is only 10. The curve for $\theta=90°$ has been scaled to fit the data.

other configurations outside the OSRPA model space. In any event, the assignment of 4^- $T=1$ to this state must be considered tentative because of the large reduction required in the calculated strength. Table VII lists the OSRPA amplitudes for the second 4^- $T=1$, which this state is conjectured to be.

If the observed resonance is the second OSRPA 4^- $T=1$ state, then where is the first 4^- $T=1$? The first OSRPA 4^- $T=1$ state has a predicted excitation energy of 15.7 MeV with approximately 25% of the maximum squared form factor of the second 4^- $T=1$. If its excitation energy is reduced by 1.0 to 2.5 MeV, as required for other even-spin magnetic transitions, then it would lie in the 13–14.5 MeV region. As can be seen from Fig. 1, there is a large number of strong excitations in this energy region, and so the first 4^- $T=1$ state may be obscured.

G. 2^- $T=1$ state

A state has been observed at $E_x=12.650\pm0.050$ MeV which corresponds to a 2^- $T=1$ state previously identified in (e,e') by Johnston and Drake[27] at $E_x=12.67$ MeV. These authors concluded that the experimental form factor was not characteristic of a single state, and that there are likely two states: 2^+ and 2^-. Indeed, a 2^+ state is known to exist at $E_x=12.74$ MeV. The results of the present experiment are plotted in Fig. 12. The $\theta=160°$ to $\theta=90°$ ratio is $R=10$, which indicates that the form factor is not purely transverse; thus the state cannot be pure 2^-. Nonetheless, the OSRPA 2^- $T=1$ squared form factor has a shape which conforms to the data remarkably well, as shown in Fig. 12. The predicted excitation energy is 13.66 MeV.

V. CONCLUSION

The OSRPA has shown a striking success in the open-shell ^{24}Mg nucleus. Of the twelve 3^- $T=0$ states calculated, all of the strength is in two states of radically different parentage. The ability of the OSRPA to predict the correct strength and shape of the 3_2^- ($K=0$) and 5_1^- ($K=0$) members of the $K=0$ band is remarkable. One is left to ponder whether the more consistent RPA calculations of Blaizot and Gogny[28] extended to ^{24}Mg will account for the quenching factor of 1.7 needed for the 3_1^- ($K=3$) band form factor (Fig. 3), as well as the quenching needed for the 6^-, 5^-, 4^-, $T=1$ resonances presented herein. These measurements clearly reveal the dominant role of simple particle-hole excitations in the formation of low-lying collective negative parity "rotational bands" in ^{24}Mg.

ACKNOWLEDGMENTS

The authors wish to thank Dr. S. S. M. Wong of the University of Toronto for providing the OSRPA programs used in this investigation, and for many enlightening discussions. This research was supported by the Natural Sciences and Engineering Research Council, Canada, and by the U.S. Department of Energy under Contract Ey-76-C-02-3069.

[1]S. Yen, R. J. Sobie, T. E. Drake, H. Zarek, C. F. Williamson, S. Kowalski, and C. P. Sargent, Phys. Rev. C 27, 1939 (1983).
[2]D. J. Rowe, Rev. Mod. Phys. 40, 153 (1968); Nucl. Phys. A107, 99 (1968); *Nuclear Collective Motion* (Methuen, London, 1970), Chaps. 13 and 14; in *Dynamic Structure of Nuclear States,* edited by D. J. Rowe, L. E. H. Trainor, S. S. M. Wong, and T. W. Donnelly (University of Toronto Press, Toronto, 1972), p. 101; D. J. Rowe, S. S. M. Wong, H. Chow, and J. B. McGrory, Nucl. Phys. A298, 31 (1978).
[3]W. Bertozzi, M. V. Hynes, C. P. Sargent, C. Creswell, P. C. Dunn, A. Hirsch, M. Leitch, B. Norum, F. N. Rad, and T. Sasanuma, Nucl. Instrum. Methods 141, 457 (1977); W. Bertozzi, M. V. Hynes, C. P. Sargent, W. Turchinetz, and C. Williamson, *ibid.* 162, 211 (1979).
[4]J. B. French, E. C. Halbert, J. B. McGrory, and S. S. M. Wong, in *Advances in Nuclear Physics 3,* edited by M. Baranger and E. Vogt (Plenum, New York, 1969).
[5]T. T. S. Kuo, Nucl. Phys. A103, 71 (1967).
[6]S. S. M. Wong, D. J. Rowe, and J. C. Parikh, Phys. Lett. 48B, 403 (1974).
[7]V. Gillet and E. A. Sanderson, Nucl. Phys. 54, 472 (1964).
[8]P. M. Endt and C. Van der Leun, Nucl. Phys. A310, 113 (1978).
[9]R. E. Tribble, T. T. Garvey, and J. R. Comfort, Phys. Lett. 44B, 366 (1973).
[10]B. H. Wildenthal (private communication).
[11]D. Branford, N. Gardner, and I. F. Wright, Phys. Lett. 36B, 456 (1971).
[12]B. Zwieglinski, G. M. Crawley, H. Nann, and J. A. Nolen, Phys. Rev. C 17, 872 (1978).
[13]B. A. Brown, W. Chung, and B. H. Wildenthal, Phys. Rev. C 21, 2600 (1980).
[14]D. J. Rowe, *Nuclear Collective Motion* (Methuen, London, 1970), Chaps. 13 and 14; D. J. Thouless, Nucl. Phys. 22, 78 (1961).
[15]H. Zarek *et al.*, Phys. Rev. Lett. 38, 750 (1977).
[16]A. Richter, Nucl. Phys. A374, 193 (1982).
[17]R. A. Lindgren, W. J. Gerace, A. D. Bacher, W. G. Love, and F. Petrovich, Phys. Rev. Lett. 42, 1524 (1979).
[18]Dean Halderson, K. W. Kemper, J. D. Fox, R. O. Nelson, E. G. Bilpuch, C. R. Westerfeldt, and G. E. Mitchell, Phys. Rev. C 24, 786 (1981).
[19]S. Yen, R. Sobie, H. Zarek, B. O. Pich, T. E. Drake, C. F. Williamson, S. Kowalski, and C. P. Sargent, Phys. Lett. 93B, 250 (1980).
[20]J. Lichtenstadt *et al.*, Phys. Rev. Lett. 40, 1127 (1978).
[21]J. Lichtenstadt *et al.*, Bull. Am. Phys. Soc. 24, 53 (1979).
[22]I. S. Towner and F. C. Khanna, Phys. Rev. Lett. 42, 51 (1979).
[23]J. Dubach and W. C. Haxton, Phys. Rev. Lett. 41, 1453 (1978).
[24]W. Weiss, Nucl. Phys. A374, 505 (1982).
[25]H. Arenhovel, Nucl. Phys. A374, 521 (1982).
[26]J. Delorme, Nucl. Phys. A374, 541 (1982).
[27]A. Johnston and T. E. Drake, J. Phys. A 7, 898 (1974).
[28]J. P. Blaizot and D. Gogny, Nucl. Phys. A284, 429 (1977).